# Phase-Contrast Magnetic Resonance Imaging Analysis of Cerebral Hyperperfusion Syndrome After Surgery in Adult Patients with Moyamoya Disease

*Feng Gao[1], Wei Zhao[1], Yu Zheng[1], Shihong Li[1], Guangwu Lin[1], Ming Ji[1], Yu Duan[2], Jian Li[2], Yanqing Hua[1]*

■ OBJECTIVE: **To investigate potential risk factors for cerebral hyperperfusion syndrome (CHS) after surgery in patients with moyamoya disease (MMD) using phase-contrast magnetic resonance imaging (MRI).**

■ METHODS: **The study included 84 adult patients (89 brain hemispheres) with MMD who underwent surgery. Preoperative phase-contrast MRI scans were performed for all patients. Peak velocity, average velocity, average flow, forward volume, and region of interest area of the bilateral internal and external carotid arteries, superficial temporal artery, and vertebral artery were calculated and analyzed. Patients were divided into CHS and non-CHS groups. Patients' age, sex, clinical symptoms, Suzuki stage, and MRI flow examination results were compared between the 2 groups.**

■ RESULTS: **Nineteen of 84 patients (89 hemispheres) with MMD were in the CHS group. Patients with ischemic onset symptoms were more likely to develop CHS after surgery ($P < 0.05$). There were no significant differences in age, sex, and Suzuki stage between the 2 groups. For surgery ipsilateral vessels, peak velocity, average flow and forward volume of superficial temporal artery and average flow of external carotid artery and region of interest area of internal carotid artery in the CHS group were significantly lower compared with the non-CHS group ($P < 0.05$). For surgery contralateral vessels, forward volume of superficial temporal artery and external carotid artery in the CHS group was significantly lower compared with the non-CHS group ($P < 0.05$).**

■ CONCLUSIONS: **Patients with MMD and ischemic onset symptoms are more likely to develop CHS after surgery. Preoperative phase-contrast MRI analysis may be helpful to predict CHS in patients with MMD after surgery.**

## INTRODUCTION

Moyamoya disease (MMD) is a chronic occlusive cerebrovascular disease of unknown etiology characterized by bilateral steno-occlusive changes at the terminal part of the internal carotid artery (ICA) and an abnormal vascular network at the base of the brain.[1] Surgical revascularization is the optimal therapeutic option for patients with MMD by improving the cerebral blood flow.[2] Revascularization surgery methods include direct bypass surgery, such as superficial temporal artery (STA)—middle cerebral artery (MCA) bypass, which can immediately increase the cerebral blood flow; indirect bypass surgery, such as encephaloduromyosynangiosis (EDMS), which can induce ingrowth of collaterals over time; and combined bypass. According to a previous study, combined STA-MCA bypass and EDMS provided efficient revascularization and reduced acute cerebral events.[3]

Hyperperfusion syndrome in MMD was first reported by Uno et al.[4] in a patient after bypass surgery in 1998. Although bypass surgery involves a relatively small amount of blood, cerebral

**Key words**
- Cerebral hyperperfusion syndrome
- Moyamoya disease
- Phase-contrast magnetic resonance imaging

**Abbreviations and Acronyms**
**CHS**: Cerebral hyperperfusion syndrome
**ECA**: External carotid artery
**EDMS**: Encephaloduromyosynangiosis
**ICA**: Internal carotid artery
**MCA**: Middle cerebral artery
**MMD**: Moyamoya disease
**MRI**: Magnetic resonance imaging
**PC**: Phase-contrast
**ROI**: Region of interest
**STA**: Superficial temporal artery
**VA**: Vertebral artery

*From the Departments of [1]Radiology and [2]Neurosurgery, Huadong Hospital Fudan University, Shanghai, China*

*To whom correspondence should be addressed: Yanqing Hua, Ph.D. [E-mail: hyq_hd@163.com]*

*Feng Gao and Wei Zhao are co—first authors.*

*Citation: World Neurosurg. (2019) 129:e48-e55.*
*https://doi.org/10.1016/j.wneu.2019.04.191*

*Journal homepage: www.journals.elsevier.com/world-neurosurgery*

*Available online: www.sciencedirect.com*

hyperperfusion syndrome (CHS) is frequently observed after revascularization surgery, particularly in adult patients.[5,6] It has been reported that patients with MMD have a significantly higher risk of CHS after bypass surgery than patients with other atherosclerotic occlusive cerebrovascular diseases.[7] Previous studies have shown that CHS is associated with morbidity and mortality,[8,9] indicating the importance of preoperative identification of CHS and appropriate management of patients at risk. CHS is mainly due to postoperative hemodynamic change, which could be identified by different imaging modalities, such as transcranial Doppler, single-photon emission computed tomography, computed tomography, and magnetic resonance imaging (MRI).[10] Transcranial Doppler is a noninvasive and portable technique; however, the thick skull bone makes accurate examination difficult or impossible, and the results are dependent on operator experience.[11,12] With respect to single-photon emission computed tomography and computed tomography perfusion examination, radiation is considered to be a major drawback. Quantitative phase-contrast (PC) MRI is a noninvasive technique that does not require a contrast agent and can measure blood vessels one by one. PC-MRI has been widely used to evaluate the carotid arteries, the vertebral artery (VA), and the cardiovascular system and has achieved promising results.[13,14] To the best of our knowledge, few studies have used this technique to quantify cerebral blood flow in patients with MMD, and no study has investigated the blood flow of the STA, which is the main target vessel of revascularization surgery. The aim of this study was to investigate the potential risk factors of CHS after surgery in patients with MMD using PC-MRI.

## MATERIALS AND METHODS

### Patients

This study was approved by the ethics committee of our hospital. Written informed consent was obtained from each patient. All experiments were performed in accordance with relevant guidelines and regulations set by the ethics committee. From July 2017 to June 2018, 84 adult patients with MMD (45 women and 39 men; mean age, 44.15 ± 11.27 years; range, 19–65 years; 89 brain hemispheres) were included in this study. All MRI examinations were performed within 1 week before surgery. MMD was diagnosed by digital subtraction angiography according to the criteria of the Research Committee on Spontaneous Occlusion of the Circle of Willis (MMD) of the Ministry of Health and Welfare, Japan.[15] Patients who were included in the study 1) were >18 years old, 2) had no MRI examination contraindications, and 3) underwent STA-MCA bypass and EDMS combined surgery. In our hospital, most patients underwent combined surgery, but only a few patients underwent EDMS surgery. Therefore, we included only patients who underwent combined surgery in this study to avoid the bias caused by different surgery types.

### MRI Examination Protocol and Image Analysis

All preoperative MRI examinations were performed with a 3T whole-body MRI scanner (MAGNETOM Skyra; Siemens Healthcare, Erlangen, Germany) using a head-neck coil. All patients were instructed to remain still and not to think about anything with eyes closed during the MRI examination. T1-weighted imaging, T2-weighted imaging, fluid attenuated inversion recovery sequence, diffusion-weighted imaging, T1 magnetization-prepared rapid acquisition gradient echo, time of flight magnetic resonance angiography, and PC-MRI were performed in this study. The detailed MRI scanning parameters are presented in Table 1. High-resolution T1-weighted images were acquired by three-dimensional magnetization-prepared rapid acquisition gradient echo sequence. We used the images of T1 magnetization-prepared rapid acquisition gradient echo to locate the three-dimensional time of flight magnetic resonance angiography sequence from the common carotid artery to the top of the skull, and then the PC-MRI sequence was positioned based on the reconstructed maximum intensity projection image of time of flight. Regarding ICA, ECA, and VA, the scan plane was placed above the

**Table 1.** Magnetic Resonance Imaging Scanning Sequences and Parameters

| | T1WI | T2WI | FLAIR | DWI | T1-MPRAGE | TOF MRA | PC-MRI (Before Scan) | PC-MRI |
|---|---|---|---|---|---|---|---|---|
| TR/TE, ms | 230/2.46 | 5000/117 | 8000/85 | 1300/62 | 2300/2.32 | 21/3.43 | 84.6/4.86 | 73.08/7.54 |
| Thickness, mm | 5 | 5 | 5 | 5 | 0.9 | 1 | 6 | 4 |
| FA, ° | 70 | 90 | 140 | 192 | 8 | 18 | 20 | 10 |
| Intersection gap, % | 30 | 30 | 20 | 30 | 50 | −18.75 | 20 | 20 |
| TA | 25 seconds | 54 seconds | 1 minute 36 seconds | 30 seconds | 5 minutes 22 seconds | 5 minutes 13 seconds | 19 seconds | 5 minutes 29 seconds |
| FOV, $cm^2$ | 22 × 22 | 22 × 22 | 22 × 22 | 24 × 24 | 26 × 26 | 22 × 22 | 34 × 34 | 18 × 18 |
| Matrix | 256 × 192 | 384 × 281 | 256 × 162 | 192 × 192 | 256 × 256 | 320 × 180 | 192 × 68 | 336 × 336 |
| Number of *b* values | NA | NA | NA | 0 and 1000 | NA | NA | NA | NA |

T1WI, T1-weighted imaging; T2WI, T2-weighted imaging; FLAIR, fluid attenuated inversion recovery; DWI, diffusion-weighted imaging; MPRAGE, magnetization-prepared rapid acquisition gradient echo; TOF, time of flight; MRA, magnetic resonance angiography; PC-MRI, phase-contrast magnetic resonance imaging; TR, repetition time; TE, echo time; FA, flip angle; TA, time of acquisition; FOV, field of view; NA, not applicable.

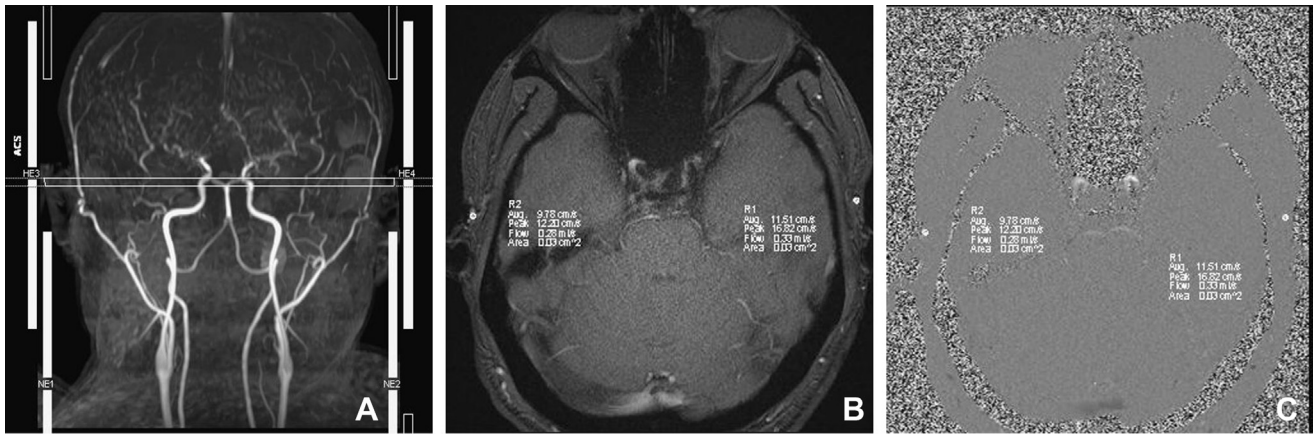


**Figure 1.** Images acquired in a representative subject illustrate the details of magnetic resonance imaging acquisition location and measurement of superficial temporal artery (STA). (**A**) Time of flight image shows the location and slice position of STA. (**B**) Magnitude image. (**C**) Phase image. R1/R2 = left/right STA. *Circles* in R1 and R2 illustrate the voxels with maximal velocities.

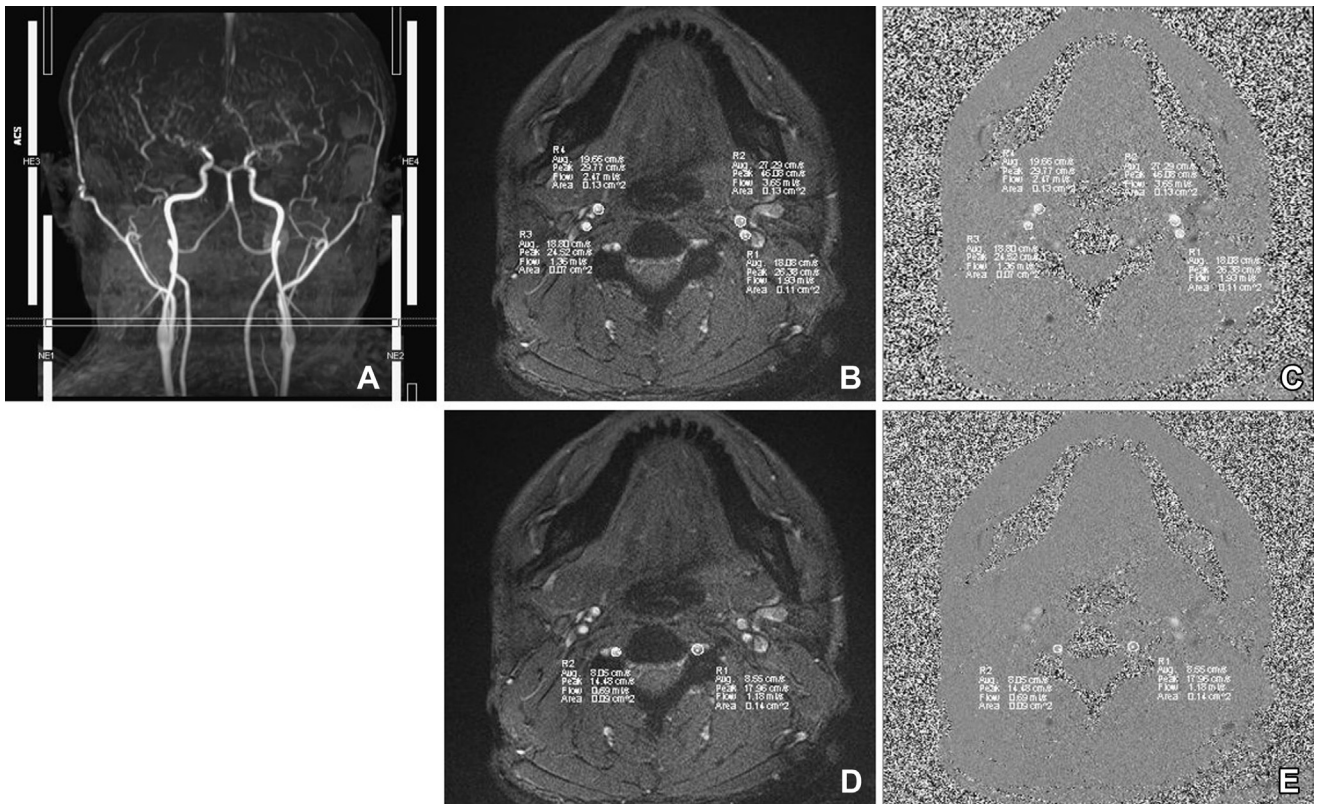


**Figure 2.** Images acquired in a representative subject illustrate the details of magnetic resonance imaging acquisition location and measurement of internal carotid artery (ICA), external carotid artery (ECA), and vertebral artery (VA). (**A**) Time of flight image shows the location and slice position of ICA, ECA, and VA. (**B**) Magnitude image. R1/R2 = left ICA/ECA; R3/R4 = right ICA/ECA. (**C**) Phase image. (**D**) Magnitude image. R1/R2 = left/right VA. (**E**) Phase image. *Circles* in R1–R4 illustrate the voxels with maximal velocities.

bifurcation of the common carotid artery. Regarding the STA, the scan plane was placed in the temporal region, and the cardiac-triggered PC-MRI scans were positioned perpendicularly to the target vessels (Figures 1 and 2). In this study, we first performed a prescan to identify the optimal velocity range of target vessels. Subsequently, we independently refined the velocity encode to obtain the best blood flow results for each patient (Table 1).

Specifically, the PC-MRI prescans of the target vessels were performed with the following velocity encoding: 10–60 cm/second (10 cm/second, 25 cm/second, 35 cm/second, 45 cm/second, 60 cm/second) for STA and 20–120 cm/second (20 cm/second, 40 cm/second, 60 cm/second, 80 cm/second, 120 cm/second) for internal carotid artery (ICA), external carotid artery (ECA), and vertebral artery (VA). As the optimal velocity range of the targeted vessels for each patient was different, we then refined the best velocity range for each patient based on the results of the prescan (the brightest sequence without any signal lost) to perform final PC-MRI. Both magnitude and phase series were loaded into the Argus Viewer (Siemens Healthcare). All flow parameters were obtained by drawing regions of interest (ROIs) on the magnitude images, which contained the lumen of the vessel as much as possible without exceeding the vessel contour (Figures 1 and 2). The ROIs drawn on the magnitude images were propagated to the phase images within the slices. Finally, the results for velocities, flows, volume, and cross-sectional areas of arteries were reported in the summary table of Argus.

### Diagnosis of CHS and Group Analysis

Symptomatic CHS was defined in this study as postoperative development of a severe headache, seizures, new neurologic deficits, and neither definite hematomas nor definite acute infarctions present on brain computed tomography, diffusion MRI, or both.[16,17] Finally, a senior neurosurgeon blinded to the study confirmed the patients with postoperative CHS. Patients were divided into a CHS group and a non-CHS group based on whether they developed CHS after surgery. We compared clinical symptoms; sex; age; hypertension; diabetes; and peak velocity, average velocity, average flow, forward volume, and ROI area of different blood vessels between the 2 groups.

### Statistical Analysis

Independent *t* test or Mann-Whitney U test, where appropriate, was used to assess the differences in continuous variables (age, peak velocity, average velocity, average flow per second, forward volume, and ROI area of the blood vessels) between the CHS group and the non-CHS group. $\chi^2$ test was used to compare the differences in categorical variables (sex, clinical symptoms, hypertension, diabetes, and Suzuki stage) between the CHS group and the non-CHS group. Receiver operating characteristic curve analysis was used to evaluate the predictive performance of the potential risk parameters between the CHS group and the non-CHS group. Statistical results were considered significant when the *P* value was $< 0.05$. Statistical analyses were performed with IBM SPSS Version 22.0 software (IBM Corporation, Armonk, New York, USA).

## RESULTS

After combined surgery, 19 of 84 patients (21.35%; 89 hemispheres) with MMD developed CHS after combined surgery. The main symptoms of CHS included severe headache (3 cases), persistent vomiting (1 case), dysphagia (3 cases), speech impairment (5 cases), muscle strength decrease (2 cases affected the upper limbs and 3 cases affected the lower limbs), and seizure (2 cases). The symptoms were observed 1–8 days (mean ± SD: 2.706 ± 1.687 days) after combined surgery. All these symptoms were improved before discharge from the hospital.

We divided the onset of clinical symptoms in patients into three groups: ischemia, hemorrhage, and nonspecific group (e.g., headache, dizziness, hand numbness, or asymptomatic). Statistically significant differences were observed between the CHS group and the non-CHS group in terms of the onset of symptoms in patients ($P < 0.05$). In the CHS group, 73.68% (14 of 19) of patients had ischemic onset symptoms, whereas 40% (28 of 70) of patients in the non-CHS group had ischemic onset symptoms. There were no statistically significant differences in age, sex, hypertension, diabetes, and Suzuki stage between the CHS group and the non-CHS group ($P > 0.05$) (Table 2).

Blood vessels were divided into ipsilateral vessels (hemispheres included with surgery) and contralateral vessels. In the CHS group, the peak velocity, average flow, and forward volume of the STA were significantly smaller compared with the non-CHS group ($P < 0.05$). In the CHS group, the average flow of the ECA was significantly lower compared with the non-CHS group, and the

**Table 2.** Clinical Characteristics in Cerebral Hyperperfusion Syndrome Group and Non–Cerebral Hyperperfusion Syndrome Group

| | CHS Group | Non-CHS Group | *P* Value |
|---|---|---|---|
| Number of patients | 19 (21.35%) | 70 (78.65%) | |
| Age, years, mean ± SD | 45.16 ± 13.59 | 43.87 ± 10.65 | 0.662 |
| Sex, male/female | 9/10 | 32/38 | 0.898 |
| Hypertension | 6 | 28 | 0.503 |
| Diabetes | 6 | 24 | 0.825 |
| Clinical symptoms | | | 0.027 |
| Ischemia | 14 | 28 | |
| Hemorrhage | 4 | 25 | |
| Nonspecific | 1 | 17 | |
| Suzuki stage | | | 0.237 |
| 1 | 0 | 0 | |
| 2 | 1 | 5 | |
| 3 | 7 | 24 | |
| 4 | 4 | 27 | |
| 5 | 5 | 13 | |
| 6 | 2 | 1 | |

CHS, cerebral hyperperfusion syndrome.

**Table 3.** Flow and Velocity Characteristics of Different Blood Vessels in Cerebral Hyperperfusion Syndrome Group and Non—Cerebral Hyperperfusion Syndrome Group

| | CHS Group | Non-CHS Group | *P* Value |
|---|---|---|---|
| Ipsilateral preoperative | | | |
| STA | | | |
| Peak velocity, cm/second | 13.877 ± 7.206 | 18.936 ± 7.416 | 0.009 |
| Average velocity, cm/second | 6.889 ± 4.889 | 8.291 ± 3.892 | 0.192 |
| Average flow, mL/second | 0.071 ± 0.535 | 0.146 ± 0.161 | 0.000 |
| Forward volume, mL | 0.045 ± 0.031 | 0.117 ± 0.104 | 0.000 |
| ROI area, $cm^2$ | 0.676 ± 0.298 | 0.555 ± 1.097 | 0.197 |
| ICA | | | |
| Peak velocity, cm/second | 25.653 ± 13.521 | 25.936 ± 10.174 | 0.921 |
| Average velocity, cm/second | 15.837 ± 9.310 | 14.319 ± 6.303 | 0.406 |
| Average flow, mL/second | 0.632 ± 0.858 | 0.941 ± 0.991 | 0.230 |
| Forward volume, mL | 0.488 ± 0.646 | 0.743 ± 0.773 | 0.247 |
| ROI area, $cm^2$ | 0.074 ± 0.174 | 0.172 ± 0.256 | 0.010 |
| ECA | | | |
| Peak velocity, cm/second | 42.365 ± 15.109 | 42.813 ± 12.982 | 0.898 |
| Average velocity, cm/second | 20.058 ± 9.287 | 18.181 ± 7.131 | 0.344 |
| Average flow, mL/second | 0.593 ± 0.470 | 1.029 ± 1.061 | 0.090 |
| Forward volume, mL | 0.456 ± 0.356 | 0.779 ± 0.697 | 0.052 |
| ROI area, $cm^2$ | 0.143 ± 0.268 | 0.106 ± 0.188 | 0.207 |
| VA | | | |
| Peak velocity, cm/second | 37.610 ± 8.232 | 34.128 ± 12.662 | 0.260 |
| Average velocity, cm/second | 22.052 ± 6.219 | 20.067 ± 14.178 | 0.555 |
| Average flow, mL/second | 0.691 ± 0.598 | 0.732 ± 0.698 | 0.936 |
| Forward volume, mL | 0.532 ± 0.448 | 0.580 ± 0.562 | 0.857 |
| ROI area, $cm^2$ | 0.073 ± 0.173 | 0.111 ± 0.226 | 0.145 |
| Contralateral preoperative | | | |
| STA | | | |
| Peak velocity, cm/second | 15.859 ± 8.112 | 20.677 ± 10.969 | 0.078 |
| Average velocity, cm/second | 7.935 ± 3.338 | 9.712 ± 5.643 | 0.194 |
| Average flow, mL/second | 0.098 ± 0.102 | 0.206 ± 0.295 | 0.055 |
| Forward volume, mL | 0.066 ± 0.062 | 0.156 ± 0.219 | 0.005 |
| ROI area, $cm^2$ | 0.571 ± 0.294 | 0.423 ± 0.389 | 0.079 |
| ICA | | | |
| Peak velocity, cm/second | 28.431 ± 12.297 | 27.540 ± 11.460 | 0.768 |
| Average velocity, cm/second | 16.226 ± 7.803 | 15.502 ± 8.119 | 0.729 |
| Average flow, mL/second | 0.544 ± 0.571 | 0.982 ± 0.987 | 0.055 |
| Forward volume, mL | 0.422 ± 0.386 | 0.771 ± 0.753 | 0.063 |
| ROI area, $cm^2$ | 0.173 ± 0.305 | 0.163 ± 0.248 | 0.145 |
| ECA | | | |
| Peak velocity, cm/second | 43.914 ± 16.056 | 42.690 ± 14.252 | 0.747 |
| Average velocity, cm/second | 19.310 ± 11.075 | 18.586 ± 7.316 | 0.735 |
| Average flow, mL/second | 0.780 ± 0.821 | 1.043 ± 1.153 | 0.398 |
| Forward volume, mL | 0.598 ± 0.540 | 0.801 ± 0.791 | 0.444 |
| ROI area, $cm^2$ | 0.043 ± 0.051 | 0.148 ± 0.248 | 0.013 |
| VA | | | |
| Peak velocity, cm/second | 34.492 ± 10.334 | 34.722 ± 11.878 | 0.939 |
| Average velocity, cm/second | 20.644 ± 8.773 | 19.129 ± 8.256 | 0.486 |
| Average flow, mL/second | 0.656 ± 0.739 | 0.812 ± 0.738 | 0.220 |
| Forward volume, mL | 0.493 ± 0.558 | 0.643 ± 0.584 | 0.170 |
| ROI area, $cm^2$ | 0.164 ± 0.303 | 0.147 ± 0.260 | 0.146 |

CHS, cerebral hyperperfusion syndrome; STA, superficial temporal artery; ROI, region of interest; ICA, internal carotid artery; ECA, external carotid artery; VA, vertebral artery.

lumen of the ICA was significantly smaller compared with the non-CHS group ($P < 0.05$) (Table 3). There were no significant differences in velocity, flow, volume, and ROI area of the ipsilateral VA between the CHS group and the non-CHS group ($P > 0.05$) (Table 3).

In the CHS group, forward volume of the STA and ECA was significantly smaller than in the non-CHS group ($P < 0.05$) (Table 3). Similarly, there were no significant differences in velocity, flow, volume, and ROI area of the ICA and VA between the CHS group and the non-CHS group ($P > 0.05$) (Table 3). The area under curve, threshold, sensitivity, specificity, and receiver operating characteristic curve of risk factors in predicting postoperative CHS are shown in Table 4 and Figure 3. Among these risk factors, the forward volume of the ipsilateral STA obtained the best predictive performance (area under curve = 0.803).

## DISCUSSION

This study showed that patients with ischemic onset symptoms were more likely to develop CHS after surgery. The patients in the

**Table 4.** Predictive Performance of Different Factors

| | AUC | Threshold | Sensitivity | Specificity |
|---|---|---|---|---|
| Peak velocity of ipsilateral STA, cm/second | 0.701 | 15.190 | 0.714 | 0.684 |
| Average flow of ipsilateral STA, mL/second | 0.772 | 0.0675 | 0.743 | 0.737 |
| Forward volume of ipsilateral STA, mL | 0.803 | 0.0585 | 0.743 | 0.737 |
| ROI area of ipsilateral ICA, $cm^2$ | 0.693 | 0.0395 | 0.614 | 0.737 |
| Forward volume of contralateral STA, mL | 0.710 | 0.0580 | 0.714 | 0.632 |
| ROI area of contralateral ECA, $cm^2$ | 0.686 | 0.0325 | 0.600 | 0.632 |

AUC, area under curve; STA, superficial temporal artery; ROI, region of interest; ICA, internal carotid artery; ECA, external carotid artery.

CHS group showed different hemodynamic changes in preoperative PC-MRI examination compared with the patients in the non-CHS group.

In patients with MMD, chronic ischemia leads to the development of new pathologic vessels, with impaired cerebrovascular autonomic regulation and cerebrovascular reactivity, and the vessels are unable to control the increased cerebral blood flow after surgery. Thus, CHS occurs after surgery.[18] The incidence of CHS in our study was 21.35% (19 of 84 patients [89 hemispheres]), which was consistent with previous studies (6.7%–38.2%).[7,19,20]

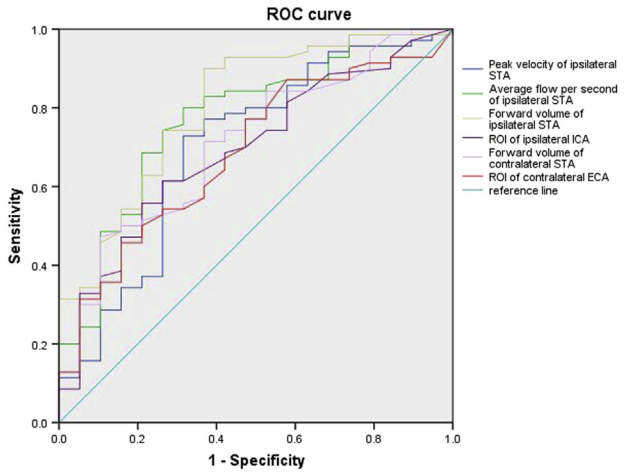


**Figure 3.** Receiver operating characteristic curve of peak velocity, average flow, forward volume of ipsilateral superficial temporal artery, region of interest area of ipsilateral internal carotid artery, forward volume of contralateral superficial temporal artery and region of interest area of contralateral external carotid artery for predicting postoperative cerebral hyperperfusion syndrome. ROC, receiver operating characteristic; STA, superficial temporal artery; ROI, region of interest; ICA, internal carotid artery; ECA, external carotid artery.

Although patients' age, sex, hypertension, and diabetes as well as Suzuki stage showed no significant differences between the CHS group and the non-CHS group in this study, the onset symptoms had statistically significant differences between the 2 groups. Previous studies demonstrated that adult patients with MMD commonly presented with hemorrhage due to intimal tearing and subsequent blood vessel rupture.[21,22]

Our study showed that approximately 32.58% (29 of 84 patients [89 hemispheres]) of adult patients presented with hemorrhage onset symptoms, but among patients with postoperative CHS syndrome, approximately 73.68% (14 of /19) of patients presented with ischemic onset symptoms, and 21.05% (4 of 19) of patients presented with hemorrhage onset symptoms. The results were consistent with a previous study, which concluded that symptomatic hyperperfusion occurred more often in patients with ischemic onset symptoms than in patients with hemorrhagic onset symptoms.[23] In contrast, Fujimura et al.[24] stated that adult patients with hemorrhagic onset symptoms are at significantly higher risk for postoperative hyperperfusion. This opposite result may be mainly due to different study populations. Our study included only adult patients, whereas the study by Fujimura et al.[24] included both pediatric and adult patients. Compensatory collateral circulation may not be well established in pediatric patients with MMD compared with adult patients with MMD. Therefore, pediatric patients may have different characteristics; this requires detailed study in the future. Meanwhile, the differences in the patient populations, surgical procedures, and preoperative management may also contribute to the discrepancy.

Previous studies mainly used perfusion imaging to evaluate postoperative CHS and demonstrated that either an increase of >100% or a comparable postoperative increase in the regional cerebral blood flow after revascularization in patients with MMD may indicate CHS.[25,26] However, those radiologic techniques could measure hemodynamics in only a specific ROI. PC-MRI can measure cerebral vessels separately. It has been applied to measure the flow rate and velocity in cerebral vasculature.[27] In this study, we used PC-MRI to evaluate not only the ICA, ECA, and VA but also the STA, which is the main target vessel of revascularization surgery.

Our study showed that the peak velocity, average flow, and forward volume of ipsilateral STA, the average flow of ipsilateral ECA, and the lumen of the ipsilateral ICA were smaller in the CHS group compared with the non-CHS group. For the contralateral hemisphere, the average flow of STA and the lumen of the ECA in the CHS group were smaller compared with the non-CHS group. Among those risk factors, the forward volume of ipsilateral STA obtained the best predictive performance (area under curve = 0.803). The STA was 1 of the terminal branches of the ECA, with a more obvious circulatory resistance. After surgery, the circulatory resistance of the distal STA can decrease[28] and thus may lead to the increased fluency of blood vessels, subsequently resulting in increased velocity and volume compared with preoperative status. In patients with a narrower ICA, the intracranial ischemia may be more severe. A sudden or substantial increased blood flow in arteries of the brain with impaired automatic adjustment due to long-term ischemia is more prone to develop CHS after surgery.[29] Moreover, the blood

supply of the ipsilateral cerebral hemisphere is more dependent on the STA after surgery.

All these changes may increase the velocity and flow volume of the STA, resulting in CHS. STA originates from the ECA, and the hemodynamic changes of STA partly reflect the homogeneous changes of ECA. Therefore, the lower peak velocity, average flow, and forward volume of the STA and ECA before surgery, the more obvious changes in terms of postoperative blood flow should be, indicating a greater chance to develop CHS. The above hypothesis may explain why patients with preoperative ECA and STA lower velocity are more likely to develop CHS after surgery in the current study.

Our results also showed that not only did preoperative ipsilateral vessels have a relationship with CHS, but also some contralateral vessels contributed to CHS, such as STA and ECA. Cerebral blood supply was supported by Willis ring, where the left and right hemispheres compensated each other, and so the contralateral blood vessels may also contribute to CHS after surgery.

In this study, the velocity, flow, volume, and ROI area of both bilateral and contralateral VAs showed no significant differences between the 2 groups ($P > 0.05$). It is known that MMD mainly affects the distal ICA and its branches, anterior cerebral artery, and MCA, whereas the posterior cerebral artery is rarely involved.[1] The target vessels of the bypass surgery are the MCA and STA and the distal branches of the ICA and ECA. The basilar artery formed by bilateral VAs is the main blood supply artery of the posterior cerebral circulation. This may explain that why the flow analysis results showed no significant differences in both bilateral and contralateral VAs between the CHS group and the non-CHS group.

The present study has several limitations. First, the sample size was small, and the number of patients who developed CHS after surgery was even smaller. Therefore, identifying independent predictors of CHS using multivariate logistic regression is not feasible. Second, CHS was diagnosed mainly based on the patient's clinical symptoms instead of the standard diagnostical method.[17,30] These clinical symptoms do not uniquely occur in CHS and may be caused by other disease. Finally, most patients who developed CHS after surgery were not deemed appropriate for the perfusion study. This will be improved in our future study.

## CONCLUSIONS

Our study shows that patients with ischemic onset symptoms are more likely to develop CHS after surgery. Preoperative PC-MRI blood flow examination may be helpful to identify patients who are at high risk to develop CHS after surgery.

## REFERENCES

1. Suzuki J, Takaku A. Cerebrovascular "moyamoya" disease. Disease showing abnormal net-like vessels in base of brain. *Arch Neurol*. 1969;20:288-299.
2. Arias EJ, Derdeyn CP, Dacey RJ, Zipfel GJ. Advances and surgical considerations in the treatment of moyamoya disease. *Neurosurgery*. 2014;74(suppl 1):S116-S125.
3. Zhao J, Liu H, Zou Y, Zhang W, He S. Clinical and angiographic outcomes after combined direct and indirect bypass in adult patients with moyamoya disease: A retrospective study of 76 procedures. *Exp Ther Med*. 2018;15:3570-3576.
4. Uno M, Nakajima N, Nishi K, Shinno K, Nagahiro S. Hyperperfusion syndrome after extracranial-intracranial bypass in a patient with moyamoya disease—case report. *Neurol Med Chir (Tokyo)*. 1998;38:420-424.
5. Fujimura M, Kaneta T, Mugikura S, Shimizu H, Tominaga T. Temporary neurologic deterioration due to cerebral hyperperfusion after superficial temporal artery-middle cerebral artery anastomosis in patients with adult-onset moyamoya disease. *Surg Neurol*. 2007;67:273-282.
6. Zhao WG, Luo Q, Jia JB, Yu JL. Cerebral hyperperfusion syndrome after revascularization surgery in patients with moyamoya disease. *Br J Neurosurg*. 2013;27:321-325.
7. Fujimura M, Shimizu H, Inoue T, Mugikura S, Saito A, Tominaga T. Significance of focal cerebral hyperperfusion as a cause of transient neurologic deterioration after extracranial-intracranial bypass for moyamoya disease: comparative study with non-moyamoya patients using N-isopropyl-p-[(123)I]iodoamphetamine single-photon emission computed tomography. *Neurosurgery*. 2011;68:957-964 [discussion: 964-965].
8. Hokari M, Kuroda S, Simoda Y, et al. Transient crossed cerebellar diaschisis due to cerebral hyperperfusion following surgical revascularization for moyamoya disease: case report. *Neurol Med Chir (Tokyo)*. 2012;52:350-353.
9. Ogasawara K, Komoribayashi N, Kobayashi M, et al. Neural damage caused by cerebral hyperperfusion after arterial bypass surgery in a patient with moyamoya disease: case report. *Neurosurgery*. 2005;56:E1380 [discussion: E1380].
10. Fujimura M, Kaneta T, Shimizu H, Tominaga T. Symptomatic hyperperfusion after superficial temporal artery-middle cerebral artery anastomosis in a child with moyamoya disease. *Childs Nerv Syst*. 2007;23:1195-1198.
11. Alexandrov AV, Sloan MA, Tegeler CH, et al. Practice standards for transcranial Doppler (TCD) ultrasound. Part II. Clinical indications and expected outcomes. *J Neuroimaging*. 2012;22:215-224.
12. Brunser AM, Mansilla E, Hoppe A, Olavarria V, Sujima E, Lavados PM. The role of TCD in the evaluation of acute stroke. *J Neuroimaging*. 2016;26:420-425.
13. Pelc LR, Pelc NJ, Rayhill SC, et al. Arterial and venous blood flow: noninvasive quantitation with MR imaging. *Radiology*. 1992;185:809-812.
14. Gatehouse PD, Keegan J, Crowe LA, et al. Applications of phase-contrast flow and velocity imaging in cardiovascular MRI. *Eur Radiol*. 2005;15:2172-2184.
15. Fukui M. Guidelines for the diagnosis and treatment of spontaneous occlusion of the circle of Willis ('moyamoya' disease). Research Committee on Spontaneous Occlusion of the Circle of Willis (Moyamoya Disease) of the Ministry of Health and Welfare, Japan. *Clin Neurol Neurosurg*. 1997;99(Suppl 2):S238-S240.
16. Iwata T, Mori T, Miyazaki Y, Tanno Y, Kasakura S, Aoyagi Y. Global oxygen extraction fraction by blood sampling to anticipate cerebral hyperperfusion phenomenon after carotid artery stenting. *Neurosurgery*. 2014;75:546-551 [discussion: 551].
17. van Mook WN, Rennenberg RJ, Schurink GW, et al. Cerebral hyperperfusion syndrome. *Lancet Neurol*. 2005;4:877-888.
18. Hayashi K, Horie N, Suyama K, Nagata I. Incidence and clinical features of symptomatic cerebral hyperperfusion syndrome after vascular reconstruction. *World Neurosurg*. 2012;78:447-454.
19. Fujimura M, Inoue T, Shimizu H, Saito A, Mugikura S, Tominaga T. Efficacy of prophylactic blood pressure lowering according to a standardized postoperative management protocol to prevent symptomatic cerebral hyperperfusion after direct revascularization surgery for moyamoya disease. *Cerebrovasc Dis*. 2012;33:436-445.
20. Kim JE, Oh CW, Kwon OK, Park SQ, Kim SE, Kim YK. Transient hyperperfusion after superficial temporal artery/middle cerebral artery bypass surgery as a possible cause of postoperative transient neurological deterioration. *Cerebrovasc Dis*. 2008;25:580-586.
21. Dusick JR, Gonzalez NR, Martin NA. Clinical and angiographic outcomes from indirect revascularization surgery for Moyamoya disease in adults and children: a review of 63 procedures. *Neurosurgery*. 2011;68:34-43 [discussion: 43].
22. Okada Y, Kawamata T, Kawashima A, Yamaguchi K, Ono Y, Hori T. The efficacy of

superficial temporal artery-middle cerebral artery anastomosis in patients with moyamoya disease complaining of severe headache. *J Neurosurg*. 2012; 116:672-679.

23. Hayashi T, Shirane R, Fujimura M, Tominaga T. Postoperative neurological deterioration in pediatric moyamoya disease: watershed shift and hyperperfusion. *J Neurosurg Pediatr*. 2010;6:73-81.

24. Fujimura M, Mugikura S, Kaneta T, Shimizu H, Tominaga T. Incidence and risk factors for symptomatic cerebral hyperperfusion after superficial temporal artery-middle cerebral artery anastomosis in patients with moyamoya disease. *Surg Neurol*. 2009;71:442-447.

25. Kaku Y, Iihara K, Nakajima N, et al. Cerebral blood flow and metabolism of hyperperfusion after cerebral revascularization in patients with moyamoya disease. *J Cereb Blood Flow Metab*. 2012; 32:2066-2075.

26. Fujimura M, Niizuma K, Endo H, et al. Quantitative analysis of early postoperative cerebral blood flow contributes to the prediction and diagnosis of cerebral hyperperfusion syndrome after revascularization surgery for moyamoya disease. *Neurol Res*. 2015;37:131-138.

27. Neff KW, Horn P, Schmiedek P, Duber C, Dinter DJ. 2D cine phase-contrast MRI for volume flow evaluation of the brain-supplying circulation in moyamoya disease. *AJR Am J Roentgenol*. 2006; 187:W107-115.

28. Fujimoto S, Toyoda K, Inoue T, Jinnouchi J, Kitazono T, Okada Y. Changes in superficial temporal artery blood flow and cerebral hemodynamics after extracranial-intracranial bypass surgery in moyamoya disease and atherothrombotic carotid occlusion. *J Neurol Sci*. 2013;325:10-14.

29. Noguchi T, Kawashima M, Nishihara M, Egashira Y, Azama S, Irie H. Noninvasive method for mapping CVR in moyamoya disease using ASL-MRI. *Eur J Radiol*. 2015;84:1137-1143.

30. Kawamata T, Kawashima A, Yamaguchi K, Hori T, Okada Y. Usefulness of intraoperative laser Doppler flowmetry and thermography to predict a risk of postoperative hyperperfusion after superficial temporal artery-middle cerebral artery bypass for moyamoya disease. *Neurosurg Rev*. 2011;34:355-362 [discussion: 362].

*Conflict of interest statement: This study was funded by the National Natural Science Foundation Project (grant number 81771816).*

*Received 11 January 2019; accepted 22 April 2019*

*Citation: World Neurosurg. (2019) 129:e48-e55.*
*https://doi.org/10.1016/j.wneu.2019.04.191*

*Journal homepage:* ***www.journals.elsevier.com/world-neurosurgery***

*Available online:* ***www.sciencedirect.com***

*1878-8750/$ - see front matter* 